Pelvic Response Investigation of Lateral Loading Conditions using Finite Element Models

Jaeho Shin, Costin D. Untaroiu, Jeff R. Crandall
University of Virginia Center for Applied Biomechanics

Abstract

Since the limited space between the car structure and an occupant makes it difficult to manage side impact energy, much biomechanical investigation has been done by subjecting the pelvis to lateral loading. In this study, the dummy finite element model was partially modified to verify the lateral pelvic loading by a rectangular shape impactor and used to explain in detail the previous investigation under iso-energy. In order to better understand the influence of impact mass and velocity under iso-energy, linear momentum and total energy conservation theories were introduced. Using driven equations from the theories and the simplified pelvis model, this study proved that the maximum internal energy levels should be different under iso-energy: the greater the impact mass, the less the internal energy level. This finding correlates with the previous pelvis loading investigation: the greater the impact mass, the less the pelvic loading, since it was shown that the impact loading is proportional to the internal energy. Thus, this study calculated the impact mass and velocity combinations to maintain the same internal energy level based on analytical solutions and finite element simulations. Closed values of the maximum pelvic forces were obtained when the calculated impact mass and velocity conditions were applied on the dummy lateral impact model. Furthermore, this methodology in conjunction with the analytical solution and the finite element simulation should be an appropriate way to set up the impact test configurations using manageable internal energy levels which may help to better understand the loading characteristics.

Introduction

While crush zones in the front of an automobile enable considerable energy absorption in frontal impacts, the limited space between the vehicle door and an occupant makes it difficult to manage the impact energy in side impacts. Thus, serious injury and mortality is a frequent consequence of side impacts. In particular, pelvic injuries resulting from automotive side impacts are associated with high mortality and morbidity, as well as substantial economic costs [1].

Biomechanical tests of the pelvis subject to lateral loading have been conducted by Cesari et al. [2], Viano [3], and Bouquet et al. [4]. In addition, sled tests that have examined pelvic loading during lateral impacts have been conducted by Pintar et al. [5] and Maltese et al. [6]. The sled tests differ from the impactor tests in that the pelvic response was coupled to the proximal and distal body parts (i.e., thorax/abdomen and lower extremities). To complement the experimental investigations, numerous pelvis models have been developed to simulate the pelvis response and injury during lateral loading [7, 8, 9, 10]. Among them, Song et al. [7] developed a three-dimensional finite element (FE) model of the pelvis and validated the human FE model against dynamic experiments on whole post mortem human subject (PMHS). They examined the influence of impact mass, velocity and surface shape on the pelvic response using the FE model.

Meanwhile, there is some disagreement between the experimental and the FE simulation results in terms of the pelvis loading characteristics. Bouquet et al. [4] provided an approach on the human pelvis tolerance against lateral impacts with PMHS. They performed impact tests with a rigid plate (200 x 200 mm) covering the whole pelvic structure so that the influence of impactor parameters could be evaluated. The impactor mass and velocity were designed in order to examine which one is dominant for a given energy level. They concluded that neither the mass nor the velocity seemed to be dominant under iso-energy based on their experimental results.

Furthermore, in their analyses, they found that, to represent vehicle side impact, the impacting mass should be lower than 23.4 kg. The 23.4 kg mass was the most frequently one used in pelvis lateral impact tests. Hence, in their conclusion, the finding that neither the mass nor the velocity seemed to be dominant under iso-energy was essential to understand pelvis behavior in new impact test conditions.

Song et al. [7] carried out a parametric analysis using the validated pelvis FE model to examine the influence of the impact mass and velocity under iso-energy conditions. Their simulations were performed with impact masses of 12 kg, 16 kg, and 23.4 kg and corresponding velocities under iso-energy. They showed the influence of the impact mass and velocity on the loading sustained by the pelvis. The pelvic response might be different according to the combination of the impact mass and velocity for identical impact energy: the greater the impact mass, the less the loading on the pelvis. Their observation was contrary to the aforementioned conclusion by Bouquet et al. [4]. In addition, they merely explained this disagreement in terms of the variability of the PMHS without discussing the physical meaning of the iso-energy condition.

Therefore, in order to clarify the disagreement between the studies of Bouquet et al. [4] and Song et al. [7], fundamental physics theories were introduced in this study for the investigation of the pelvic loading characteristics under iso-energy. Before observing the impact loading characteristics in detail, the Hybrid-III FE dummy was chosen and verified against given published data. Based on dummy lateral impact simulations considering different impact masses and velocities under iso-energy, internal energies of the impact models, velocities of the pelvis and the impactor, and contact forces were calculated and compared. Specifically, the internal energy was considered when investigating the loading characteristics, since impact loading is a function of the internal energy [11]. Then, the relationship between the internal energy and the initial condition (masses and velocities) was studied using an analytical solution and a simplified pelvis model. Finally, additional simulations using the Hybrid-III dummy model were performed to investigate the pelvic loading characteristics practically.

Hybrid-III FE Model

In this study, the Hybrid-III FE model provided by Livermore Software Technology Corporation (LSTC) was used for pelvis response investigations. The dummy FE model consists of 99 deformable and rigid parts that are connected together using different joint definitions [12]. The model contains nearly 5,980 elements.

Figure 1 shows the model set-up simulating the lateral impact test configuration impacted by the rigid impactor. The impactor model is the same size (200 x 200 mm) as the impactor used in the previous publications [4, 7]. The computer simulation works were carried out using the commercial explicit code, LS-DYNA®. Since the Hybrid-III FE model is known as merely having sufficient compatibility of frontal crash test configurations, it was necessary to modify and verify the dummy model used for lateral impact loading. The FE model modification was conducted in terms of the lateral thickness of the pelvis flesh. The pelvis model was remodeled to increase the flesh lateral thickness, to 80 mm, since the overall flesh thickness of the 50th percentile male FE model is around 80 mm in a lateral side [13].

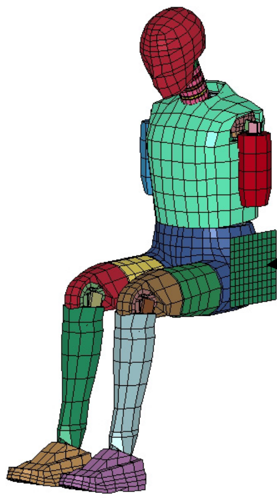

Figure 1: The model set-up simulating the lateral impact test.

Verification Study of Hybrid-III Dummy Model

The material identification simulation was performed so that the lateral impact response of the Hybrid-III FE model could be verified against the data published by Song et al. [7]. Based on the published simulation model [7], the dummy model was impacted with the 200 x 200 mm impact surface under 131 J iso-energy configurations (three different mass and velocity combinations) as shown in Table 1. For a given low density foam material model (material type 57 for modeling highly compressible low density foams) of the pelvis flesh, iterative identification of the specific stress-strain curves, as shown in Figure 2(a), used in the simulation was performed to match maximum loading levels provided by Song et al. [7]. Figure 2(b) compares the lateral loading response under 131 J iso-energy configurations between the final simulation results of the iterative runs and the published peak force data [7]. The results showed good correlation between them in terms of the peak force levels.

Table 1: The simulation matrix for the influence examination of impact mass and velocity under 131 J and 510 J iso-energy conditions.

Energy	Mass & Velocity I	Mass & Velocity II	Mass & Velocity III
131 J	12.0 kg – 4.68 m/s	16.0 kg – 4.05 m/s	23.4 kg – 3.35 m/s
510 J	12.0 kg – 9.22 m/s	16.0 kg – 7.98 m/s	23.4 kg – 6.60 m/s

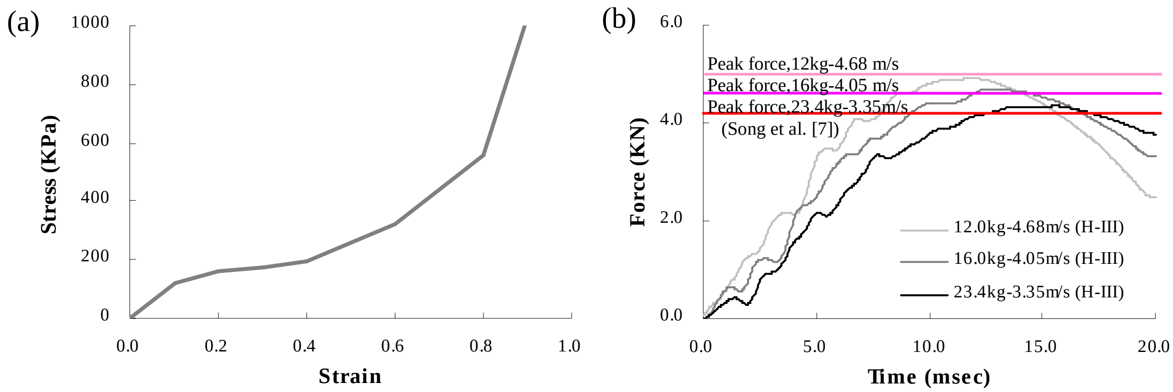

Figure 2: Stress-strain curve of the pelvis flesh material obtained from iterative simulations (a) and force-time curves of pelvis lateral impact simulations (b).

Pelvic Loading Simulation Under Iso-energy

Using the verified Hybrid-III FE model in the lateral pelvic loading, the dummy model was impacted again with the same impactor shape to examine the influence of impactor mass and velocity under a higher iso-energy (510 J) configuration. Since the impact simulation had been performed under 131 J iso-energy level in the previous section, another iso-energy level based on the previous study [7] was chosen to evaluate the influence of the impact mass and velocity under two different iso-energy levels. Table 1 shows the simulation matrix designed to examine the influence of impact mass and velocity under iso-energy conditions. In order to investigate the influence of impact mass and velocity in detail, the energy-time, the velocity-time, and the contact force-time curves were plotted and compared under two different iso-energy conditions.

First, in kinetic and internal energy comparisons of pelvis impact models, the model employing the “12.0 kg – 4.68 m/s” input conditions showed the lower minimum level of its kinetic energy curve and the higher peak level of its internal energy curve and the “23.4 kg – 3.35 ms” input model shows opposite trends (Figure 3(a)), although the total energies are the same as 131 J. Likewise, we obtained similar results under 510 J iso-energy condition as shown in Figure 3(b). Second, the velocity time histories of the impactor and the pelvis mass center were compared. The common velocity, when two centers of the impactor and the pelvis approach with a minimum distance, was smaller in the “12.0 kg – 4.68 m/s” input model and appeared at the earlier time notwithstanding same total energies as 131 J (Figure 3(c)). Under 510 J iso-energy conditions, the similar velocity plots were observed as shown in Figure 3(d). Finally, when we plotted the contact force-time curves for each case, the higher peak value appeared in the simulation model of the “12.0 kg – 4.68 m/s” input configuration rather than the “16.0 kg – 4.05 ms” and the “23.4 kg – 3.35 ms” simulation models (Figure 3(e)). Furthermore, the similar plot patterns were calculated in the high level iso-energy conditions as shown in Figure 3(f). Through the internal energy and the contact force time histories, the peak values of the internal energy and the contact force were observed when the common velocities were obtained in each mass and velocity configuration. This observation that the peak levels of the internal energy and force were obtained at same times could be explained instinctively by a physical point of view. In addition, Figure 4 shows the influence of the impact mass and velocity on the pelvic loading. Each increase rate is different according to the mass of impactor. Since the peak level of impact force depended on the impact mass, this result of the lateral impact simulations showed similar trends to the results of the previous study performed by Song et al. [7]: the greater the impact mass, the less the loading on the pelvis.

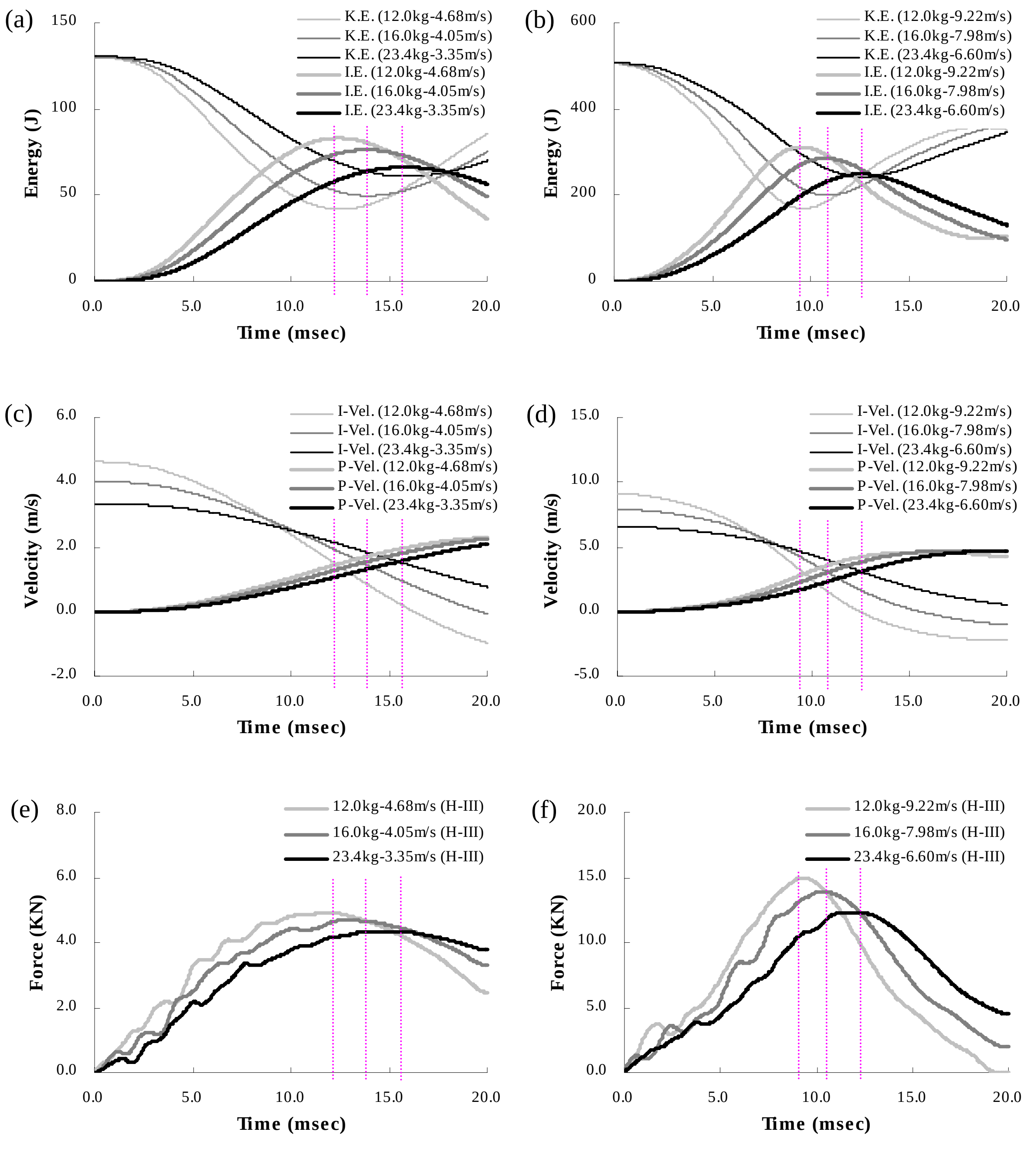

Figure 3: Time history plots for internal and kinetic energies of the 131 J iso-energy configuration (a) and the 510 J iso-energy configuration (b), impactor and pelvis velocities of the 131 J iso-energy configuration (c) and the 510 J iso-energy configuration (d), and contact forces of the 131 J iso-energy configuration (e) and the 510 J iso-energy configuration (f).

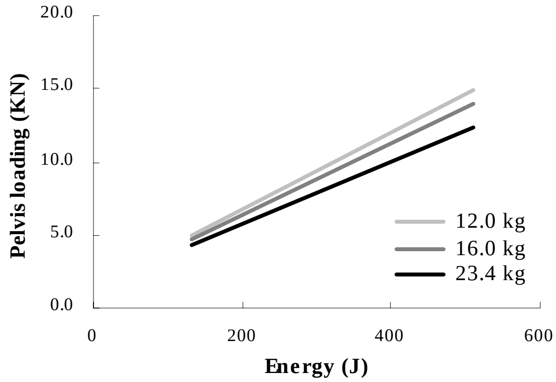

Figure 4: Influence of impact mass and velocity on the pelvis loading under iso-energies.

Analytical Approaches

Although the same kinetic energies of impactors were applied to the Hybrid-III FE model, different impact forces and internal energy levels were observed during previous simulations. Therefore, the linear momentum and the total energy conservations were introduced in a simple analytical impact model.

Since the impacted pelvis model might be simplified using the interaction model with two objects in one dimension illustrated in Figure 5, where the two objects are referred to as the impactor and the Hybrid-III pelvis model. The velocity of the impactor is represented by the time dependent variable V_1, while that of the dummy pelvis is represented by V_2. As the impactor moves into interact with the dummy pelvis, the contact force develops, which is represented by the time-dependent variable F.

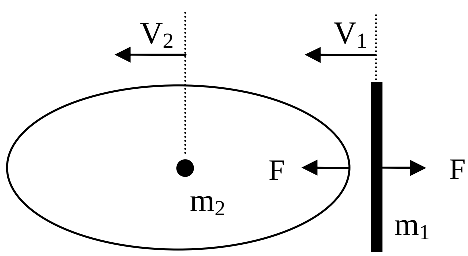

Figure 5: The simplified impact model drawing of the dummy pelvis and the impactor models.

Based on the simple impact model, we can obtain the well-known equation of the linear momentum conservation [11],

$$m_1 V_{1(t=0)} + m_2 V_{2(t=0)} = m_1 V'_{1(t=T)} + m_2 V'_{2(t=T)} \quad (1)$$

where T is an arbitrary time during the whole impact period.

Then, the velocity of the mass center of the system can be expressed,

$$V_{cm} = \frac{m_1 V_{1(t=0)} + m_2 V_{2(t=0)}}{m_1 + m_2} = \frac{m_1 V'_{1(t=T)} + m_2 V'_{2(t=T)}}{m_1 + m_2} \quad (2)$$

Since the initial velocity of the pelvis is zero in the simple impact model, $V_{2(t=0)} = 0$. When $V'_{1(t=T)}$ is same as $V'_{2(t=T)}$ at time, T (at maximum closure between two objects), the common velocity of the impact model is

$$V_{cm} = \frac{m_1}{m_1 + m_2} V_{1(t=0)} = \frac{m_1 V'_{1(t=T)} + m_2 V'_{2(t=T)}}{m_1 + m_2} = V'_{1(t=T)} = V'_{2(t=T)} \tag{3}$$

During closure between the two objects, as the center of the impactor continue to approach to the center of the pelvis model the internal energy is absorbed as work done to the impacted pelvis. When the objects achieve common velocity, the closure is complete. Hence, during the closure phase of the impact model, the absorbed internal energy is evaluated as [11],

$$T.E. = K.E + I.E.,\ \ I.E. = T.E. - K.E = \frac{1}{2} m_1 (V^2_{1(t=0)} - V^2_{cm}) + \frac{1}{2} m_2 (V^2_{2(t=0)} - V^2_{cm}) \tag{4}$$

Since $T.E.$ is the total energy and $K.E.$ represents the kinetic energy of the impact model at the closure phase, the equation 4 shows the total energy conservation in the system. If $V_{2(t=0)} = 0$ for the pelvis impact model,

$$I.E. = \frac{1}{2} m_1 (V^2_{1(t=0)} - V^2_{cm}) + \frac{1}{2} m_2 (V^2_{2(t=0)} - V^2_{cm}) = \frac{1}{2} m_1 V^2_{1(t=0)} - \frac{1}{2} (m_1 + m_2) V^2_{cm} \tag{5}$$

Using the equation 3, the equation 5 can be simplified, as

$$I.E. = \frac{1}{2} m_1 V^2_{1(t=0)} \left(\frac{m_2}{m_1 + m_2} \right) = T.E. \left(\frac{m_2}{m_1 + m_2} \right) \tag{6}$$

The equation 6 shows the maximum internal energy is the function multiplying the total energy by the mass ratio of the pelvis mass and the total mass of the impact model.

On the other hand, for the impactor and the pelvis models, the relationship between impact force, F, and displacement, u is

$$F = ku \tag{7}$$

assuming the linear force displacement relation associate with the impact model [11], then the internal energy is

$$I.E. = \int F du = \frac{1}{2} F u = \frac{1}{2} \frac{F^2}{k} \tag{8}$$

where k is a contact stiffness between the impactor and the simplified pelvis model. Finally, we obtained the internal energy is the function of masses of two objects and is represented by the contact force and the stiffness of the impact model using the equation 6 and 8 simultaneously. Hence, the impact force levels should be different with the different impact masses and velocities under iso-energy. The fundamental reason is that impact force is in proportion to the internal energy which is dominant with the typical mass ratio, $\{m_2/(m_1 + m_2)\}$, based on the equation 6.

Simplified Pelvis FE Model

Based on the previous analytical approaches, the simplified FE pelvis model was used to compare results from the analytical solutions and the FE simulations and to verify the relationships with the internal energies and the impact forces. Figure 6 shows the simplified pelvis FE model from the Hybrid-III dummy model. The adjustable mass was applied on the mass center of the pelvis to meet total impacted mass, as 25 kg, because the overall mass of the pelvis part is around 25 kg in the Hybrid-III dummy FE model. The pelvis center was constrained in all translations and rotations except in one translation of the impacting direction to employ the linear momentum theory. Similarly, the simplified pelvis model was impacted with the same impactor model (the model dimension: 200 x 200) under 131 J iso-energy configuration (Table 1). In the simulation results, the kinetic and the internal energies, the velocities at the maximum closure between two objects, and the contact forces were calculated and compared with them obtained by the analytical solutions. After the first simulation series under iso-energy, the second impact simulation series was performed to obtain the close loading levels based on the same internal energy conditions. Figure 7 shows the basic idea of FE simulations under iso-energy and in the same internal energy for the simplified pelvis model.

In the resulting comparisons, first, the common velocities and the maximum internal energies were calculated using the analytical solutions (equation 3 and 5) and the pelvis impact simulations for each mass and velocity combination. Overall good agreements were obtained between the analytical and the simulation results as the maximum difference was around 2.7 % in internal energy level comparisons (Table 2). The summarized table, Table 2, showed different internal energy levels under iso-energy as expected previous observations. For identical impact energy, the internal energy levels are different according to the combination of the impact mass and velocity: the greater the impact mass, the less the internal energy. The peak force levels were also different related on the combination of the impact mass and velocity as shown in Figure 8(a). The force-time curves show a similar trend to the internal energy time histories: the greater the impact mass, the less the contact force, since the contact force is able to be represented by a proportional function of the internal energy.

Bouquet et al. [4] made efforts to define a new pelvic impact test configuration, because the impactor mass should be lower than the 23.4 kg in their finding. However, their new configuration was only based on the same total energy level. Thus, in this study, the identical impact velocities for a reduced mass set (12.0 kg and 16.0 kg) were considered as being able to maintain the internal energy level of the "23.4 kg – 3.35 ms" model (Table 3). The calculated impact velocities were 4.09 m/s for 12.0 kg and 3.73 m/s for 16.0 kg using the equation 3, 5, and 6 inversely. Then, the second impact simulation series was performed using updated mass-velocity combinations such as "12.0 kg – 4.09 m/s" and "16.0 kg – 3.73 m/s". Figure 8(b) shows the contact force curves in maintaining the internal energy levels. When the updated mass-velocity set was applied to the simplified impact model, much closer peak force levels were obtained as compared to the target force level of the "23.4 kg – 3.35 ms" combination.

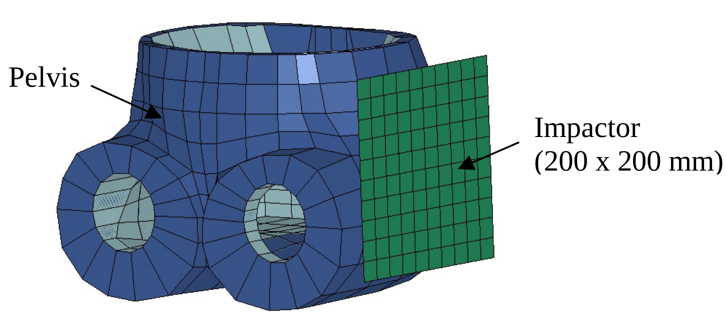

Figure 6: The simplified pelvis impact model.

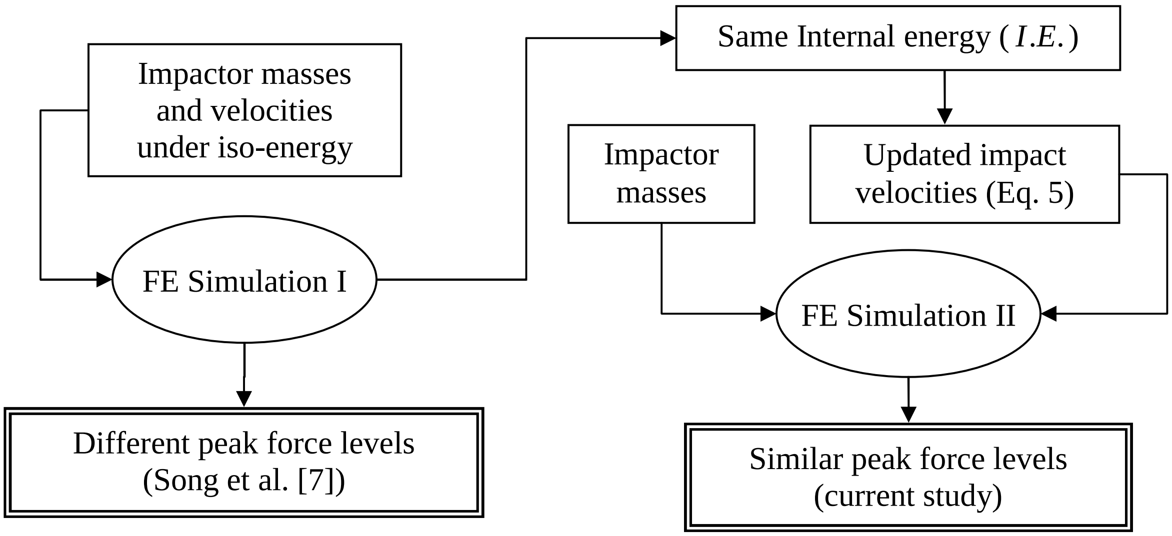

Figure 7: Schematic flow chart of the FE simulations for the simplified pelvis model.

Table 2: Identified common velocities and maximum internal energies using analytic calculations and FE simulations under 131 J iso-energy configurations.

Input parameters				Output 1		Output 2	
Total energy ($T.E.$, J)	Mass (kg)		Initial impact velocity ($V_{1(t=0)}$, m/s)	Common velocity (m/s)		Maximum Internal energy ($I.E.$, J)	
	Impactor (m_1)	Pelvis (m_2)		Analytic calculation by Eq. 3 (V_{cm})	FE simulation (V'_{cm})	Analytic calculation by Eq. 6	FE simulation
131	12.0	25.0	4.68	1.52	1.51	88.5	86.4
	16.0	25.0	4.05	1.58	1.59	79.9	78.9
	23.4	25.0	3.35	1.62	1.60	67.8	66.9

Table 3: Identified common velocities and initial impact velocities to maintain the internal energy, 67.8J.

Input parameters			Output 3	Output 4
Maximum Internal energy ($I.E.$, J)	Masses (kg)		Common velocity by Eq. 3 & 5 (V_{cm} , m/s)	Initial impact velocity by Eq. 6 ($V_{1(t=0)}$, m/s)
	Impactor (m_1)	Pelvis (m_2)		
67.8	12.0	25.0	1.33	4.09
	16.0	25.0	1.45	3.73
	23.4	25.0	1.62	3.35

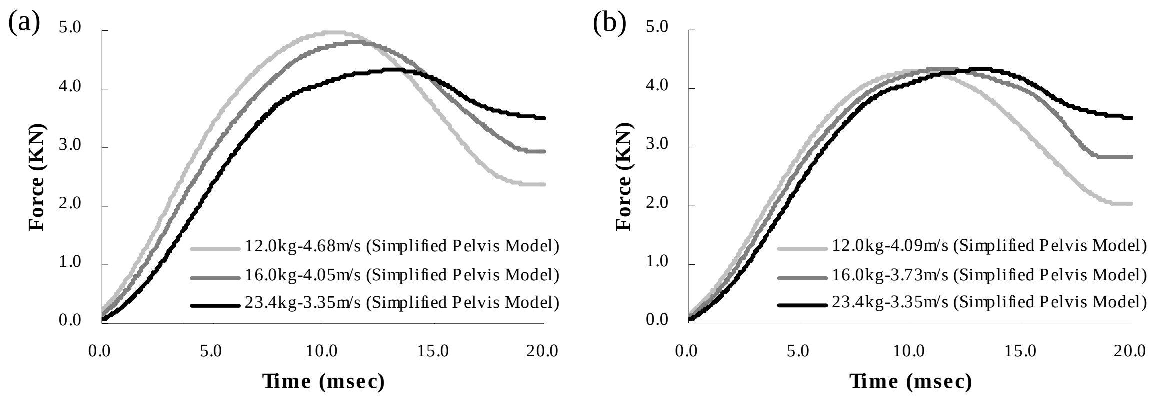

Figure 8: Pelvic loading time histories under iso-energy (a) and in keeping internal energy levels (b).

Analysis of Pelvic Lateral Loading Response

Finally, Hybrid-III lateral impact simulations were performed again to reveal the pelvic loading characteristics of a whole body model. The simulation results were compared with the analytical solutions based on fundamental physics approaches. However, the previous consideration is limited to assume the linear momentum conservation with the fully overlap impactor model whose impact force could be transferred to the impacted body thoroughly without rotational modes. Hence, this study considered the effective pelvis mass referred to by Chi and Schmitt [14] in order to apply previously discussed analytical approaches to the whole body model. Chi and Schmitt [14] introduced two different definitions of the effective mass such as the work-energy method (WEM) and the impulse-momentum method (IMM). Theoretically, WEM and IMM are equivalent and should yield the same results for effective mass. However, IMM may be more accurate than WEM, since IMM only needs maximum deformation instead of precisely synchronized force-displacement data, when applied to moving subjects [14]. Based on their approaches, the impulse-momentum method was used to calculate the effective pelvis mass of the Hybrid-III FE model. Therefore, the effective pelvis mass can be calculated as,

$$m_{effective-pelvis} = m_1\left(\frac{V_{1(t=0)}}{V'_{cm}} - 1\right) \tag{9}$$

where V'_{cm} is calculated by FE simulation. Since there are two unknown parameters (the common velocity and the effective mass) in equation 5, it is impossible to calculate both directly using analytic equations only. Thus, the common velocity was determined by the FE simulation showing good agreement with the analytical solution in the previous section. Then, we can rewrite equation 5 in terms of the effective pelvis mass, $m_{effective-pelvis}$ and the common velocity, V'_{cm},

$$I.E. = \frac{1}{2}m_1 V_{1(t=0)}^2 - \frac{1}{2}(m_1 + m_{effective-pelvis})V'^2_{cm} \tag{10}$$

In the previous simulation results under iso-energies, 131 J and 510 J, the common velocities were chosen from the velocity-time history curves calculated by FE simulations (Figure 3(d)). Then, each effective mass and the maximum internal energy were calculated using equation 9 and 10, and the calculated internal energy levels were compared with the maximum internal energies obtained by the Hybrid-III lateral impact simulations. Table 4 shows good agreements between the analytic calculation results and the simulation results with regard to internal energy levels. Both calculation results provided the similar output trend as shown Table 2 for simplified pelvis impact models: the less the initial velocity, the less the internal energy under iso-energy.

Using a similar procedure, the identical impact velocities for each mass condition were calculated to maintain the target values of the internal energy, 70.9 J, from the "23.4 kg – 3.35 m/s" and the 271 J from the "23.4 kg – 6.60 m/s" input sets (Table 5). Then, the dummy lateral impact simulations were performed again according to updated mass-velocity combinations such as "12.0 kg – 4.14 m/s" and "16.0 kg – 3.75 m/s". In the simulation results, Figure 9 shows the comparisons of the force time histories under 131 J (Figure 9(a)) and in maintaining the internal energy, 70.9 J (Figure 9(b)). In addition, the force-time curves under 510 J and in keeping the internal energy, 271 J, were shown in Figure 10. In the same manner, when modified mass-velocity sets were applied on the dummy lateral impact model, closer peak force levels were obtained in comparisons with the target results.

Table 4: Identified common velocities, effective pelvis masses, and maximum internal energies using analytic calculations and FE simulations under iso-energy configurations.

Input parameters			Output 5	Output 6	Output 7	
Total energy ($T.E.$, J)	Impactor mass (m_1, kg)	Initial impact velocity ($V_{1(t=0)}$, m/s)	Common velocity by FEM (V'_{cm}, m/s)	Effective pelvis mass by Eq. 9 ($m_{effective-pelvis}$, kg)	Maximum Internal energy by Eq. 10 ($I.E.$, J)	Maximum Internal energy by FEM ($I.E.$, J)
131	12.0	4.68	1.45	26.73	90.7	88.4
	16.0	4.05	1.51	26.91	82.3	80.7
	23.4	3.35	1.54	27.50	70.9	69.7
510	12.0	9.22	2.93	25.76	348.0	336.4
	16.0	7.98	3.03	26.14	316.0	306.5
	23.4	6.60	3.09	26.58	271.0	264.7

Table 5: Identified common velocities and initial impact velocities to maintain the internal energies, 70.9 J and 271 J.

Input parameters		Output 6 from Table 4	Output 8	Output 9
Maximum Internal energy ($I.E.$, J)	Impactor mass (m_1, kg)	Effective pelvis mass ($m_{effective-pelvis}$, kg)	Common velocity by Eq. 9 & 10 (V'_{cm}, m/s)	Initial impact velocity by Eq. 9 & 10 ($V_{1(t=0)}$, m/s)
70.9	12.0	26.73	1.28	4.14
	16.0	26.91	1.39	3.75
	23.4	27.50	1.54	3.35
271	12.0	25.76	2.56	8.13
	16.0	26.14	2.79	7.38
	23.4	26.58	3.09	6.60

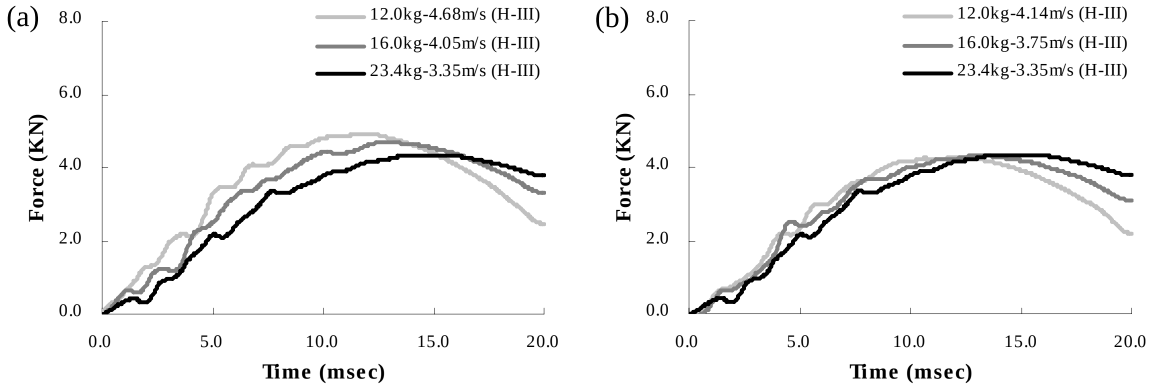

Figure 9: Pelvic loading time histories under 131 J impact energy (a) and in keeping 70.9 J internal energy (b).

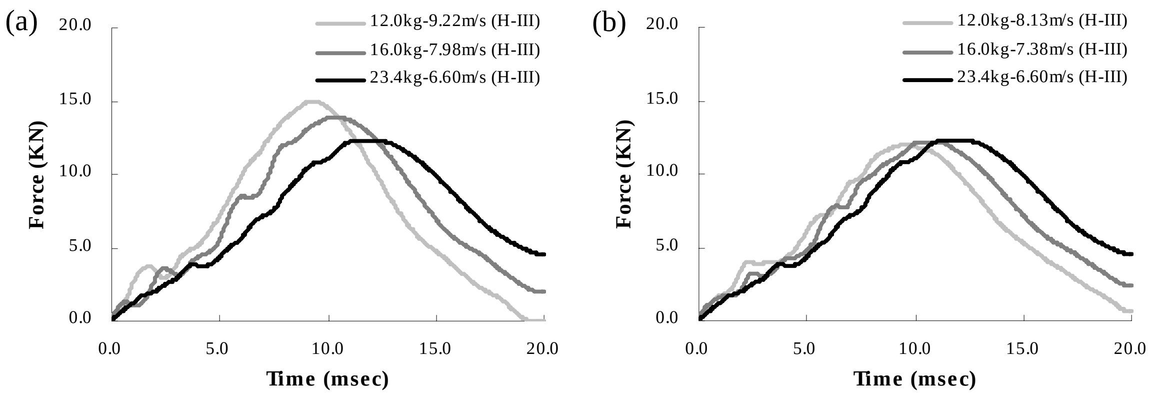

Figure 10: Pelvic loading time histories under 510 J impact energy (a) and in keeping 271 J internal energy (b).

Discussion

The objective of this study was to investigate the pelvic loading response under iso-energy conditions, since disagreement concerning of pelvic loading characteristics was observed between previous publications. The analytical approach and FE simulations were used for the investigation of the lateral loading characteristics under iso-energy configuration and showed a good correlation with the corresponding results. Although the same total energy, the iso-energy, was applied on the pelvis impact model, this study showed that the impact force levels of each impact mass-velocity configuration should be different based on the linear momentum and the total energy conservation theories. Furthermore, this study recommends updating the mass-velocity configurations to maintain the similar impact force levels. Since the impact mass should be lower than the 23.4 kg impactor on the lateral pelvic impact test [4], this finding is very useful to determine the test conditions for pelvis impact experiments.

While the Hybrid-III FE model has limited capability for the lateral loadings, it is sufficient to show the reasonable loading characteristics through the model modification and verification. Therefore, the dummy FE model provided very close result sets compared with the analytical solution, as a 3 % maximum difference.

The angular momentum theory was not considered to simplify formulations in the analytical approach, thus the simplified pelvis FE model was assumed to constrain in all rotations and translations except the one translation in the impacted direction. It is necessary to employ momentum conservations in the all directions and study the influence in future work, while the influence seems to be relatively small.

It was observed that the impact force levels should be different under iso-energy. The fundamental reason is that the impact force is in proportion to the internal energy which is only dominant with the typical mass ratio times the initial (total) energy (equation 6). Based on the relationship, if the mass of the impacted object is relatively too big, the maximum internal energy is almost close to the initial (total) energy. On the other hand, if the mass of the impacted object is relatively too small, the impactor mass plays a role in determining the internal energy levels. Therefore, it would be essential to study the given mass ratio to influence the internal energy and the impact loading.

In these local impact tests (the pelvis lateral loading test, the head impact test, and the ribcage central impact test with linear impactors), the effective mass at the interested part should be considered to evaluate the loading characteristics. However, it is difficult to calculate the effective mass of the interested location directly, since the common velocity of an impact model is unknown as well before testing. Therefore, in this study, the common velocity was chosen in the velocity-time history provided by FE simulations and an effective mass was calculated using the common velocity. This approach would be a possible way to determine the effective mass for the impact test set-up before trial experiments. Furthermore, in order to determine the unknown initial impact velocity, we used the given effective masses from the known initial impact conditions, since the variation of calculated effective masses is smaller than ±0.4 kg in this study. While the variation of effective masses is relatively small, the appropriate calculation methods for each effective mass would be discussed to obtain more accurate results, since the effective mass is varied by the initial impact velocity and the mass of the impactor.

Conclusion

The Hybrid-III FE model was modified partially to verify lateral pelvic loading and used to investigate the lateral loading characteristics under iso-energy. The dummy FE model showed a similar pelvic loading pattern to the published results under iso-energy [7]: the greater the impact mass, the less the pelvic loading. In order to evaluate the influence of the impact mass and velocity under iso-energy, fundamental physics theories were introduced in this study. Using driven equations and the simplified pelvis FE model, this study proved that the maximum internal energies should be different under iso-energy: the greater the impact mass, the less the internal energy level. Since the impact loading is proportional to the internal energy, the finding of this study is able to substantially correlate with the previous published result: the greater the impact mass, the less the pelvic loading under iso-energy. Thus, this study updated the impact mass and velocity combinations to keep the same internal energy using the analytical solution and FE simulations. Finally, we obtained very close impact loading levels, when the updated combinations were applied on the dummy model. Hence, this study strongly recommended the modified mass-velocity configurations to be able to maintain the similar pelvic loading levels. Furthermore, this methodology collaborating with the analytical solution and the FE simulation should be acceptable to set up other impact test configurations using manageable internal energy levels.

References

[1] D. P. Beason, G. J. Dakin, R. R. Lopez, J. E. Alonso, F. A. Bandak, and A. W. Eberhardt, "Bone mineral density correlates with fracture load in experimental side impacts of the pelvis," Journal of Biomechanics, vol. 36, pp. 219-227, 2003.
[2] D. Cesari and M. Ramet, "Pelvic tolerance and protection criteria in side impact," Stapp Car Crash Journal, vol. 26, pp. 145-155, 1982.
[3] D. Viano, "Biomechanical responses and injuries in blunt lateral impact," Stapp Car Crash Journal, vol. 33, pp. 113-141, 1989.
[4] R. Bouquet, M. Ramet, F. Bermond, Y. Caire, Y. Talantikite, S. Robin, and E. Voiglio, "Pelvis human responses to lateral impact," ESV conference, 1998.
[5] F. Pintar, N. Yoganandan, M. H. Hines, M. R. Maltese, J. D. Mcfadden, R. A. Saul, R. H. Eppinger, N. Khaewpong, and M. Kleinberger, "Chestband analysis of human tolerance to side impact," Stapp Car Crash Journal, vol. 41, pp. 113-141, 1997.
[6] M. R. Maltese, R. H. Eppinger, H. H. Rhule, B. R. Donnelly, F. A. Pintar, and N. Yoganandan, "Response Corridors of human surrogates in lateral impacts," Stapp Car Crash Journal, vol. 46, pp. 321-351, 2002.
[7] E. Song, X. Trosseille, and H. Guillemot, "Side impact: Influence of impact conditions and bone mechanical properties on pelvic response using a fracturable pelvis model," Stapp Car Crash Journal, vol. 50, pp. 75-95, 2006.
[8] F. Renaudin, H. Guillemot, F. Lavaste, and W. Skalli, "A 3D finite element model of pelvis in side impact," Stapp Car Crash Journal, vol. 37, pp. 249-259, 1993.
[9] B. Besnault, H. Guillemot, S. Robin, F. Lavaste, and J. Y. Le Coz, "A parametric finite element model of the human pelvis," Stapp Car Crash Journal, vol. 42, pp. 33-45, 1998.
[10] Z. Li, J. E. Kim, J. S. Davidson, B. S. Etheridge, J. E. Alonso, and A. W. Eberhardt, "Biomechanical response of the pubic symphysis in lateral pelvic impacts: A finite element study," Journal of Biomechanics, vol. 40, pp. 2758-2766, 2007.
[11] N. J. Carpenter and J. B. Welcher, "Stiffness and crush energy analysis for vehicle collision and its relationship to barrier equivalent velocity (BEV)," Society of Automotive Engineers, 2001-01-0500, 2001.
[12] A. Noureddine, A. Eskandarian, and K. Digges, "Computer modeling and validation of a Hybrid-III dummy for crashworthiness simulation," Mathematical and Computer Modeling, vol. 35, pp. 885-893, 2002.
[13] E. Haug, H. Choi, S. Robin, and M. Beaugonin, "Human models for crash and impact simulation," Handbook of Numerical Analysis, vol. 12, pp. 231-452, Elsevier, New York, NY, 2004.
[14] K. J. Chi and D. Schmitt, "Mechanical energy and effective foot mass during impact loading of walking and running," Journal of Biomechanics, vol. 38, pp. 1387-1395, 2005.